Research Article

Journal of Environmental Nanotechnology

Effect of Complex Phase Plate on Tight Focusing of Azimuthally Polarized Dark and Anti-dark Gaussian Beam

J. William Charles[1], M. Udhayakumar[1], K. B. Rajesh[1*], A. Mohamed Musthafa[2]

[1]Department of Physics, Chikkanna Government Arts College, Tiruppur, TN, India

[2]Department of General Studies, Jubail University College, Royal Commission of Jubail, Saudi Arabia

Received: 21.08.2019 Accepted: 25.09.2018 Published: 30-09-2019

*rajeshkb@gmail.com

ABSTRACT

This study was focused on azimuthally polarized Dark and Anti-dark Gaussian (DADG) beams passing through a high numerical aperture lens (NA). The Vector Diffraction theory was used to study the lens theoretically. It was reported that with appropriate phase modulation of the input DADG beam, the intensity distribution of the focused region can be modified to be a focal hole segment with numerous focal holes separated by varied axial distances. A chain of focal hole segments like this can be used for multiple trapping of low refractive index particles as well as an erase beam for STED microscopy with a high screening rate.

Keywords: Flattops; Optical tubes; Optical bubbles; Three-dimensional optical tube.

1. INTRODUCTION

A wide range of applications, including dark optical traps for atoms and manipulation (Friedman *et al.* 2002), guiding and binding of microparticles and biological cells (Mizmar *et al.* 2010) and erase beams for super-resolution fluorescence microscopy (Cizmar *et al.* 2010; Watanabe *et al.* 2003), have recently driven the generation of three-dimensional (3D) optical tube beams, which are dark regions in space surrounded by light. However, the most current technology of producing such optical tubes exhibits significant fluctuations due to unexpected diffraction. In addition, the DOE (Diffractive optical element) in the pupil plane is utilised to generate focus structures such as optical tubes, flattops and optical bubbles, which are useful for optical trapping and manipulation (Grimm *et al.* 2000; Tian and Pu, 2011; Lalithambigai *et al.* 2012). To establish a stable particle trap and transport particles with low and high refractive indexes, dissimilar optical gradient forces are necessary, and the scattering force considered is always proportional to optical intensity. Three-dimensional (3D) multi-site optical trapping requires a large number of concentrated spots in the focal region for high refractive index particles and a large number of focal holes for low refractive index particles, which is challenging to produce. A number of approaches for building multiple optical traps have been published; for example, a phase-contrast method for generating an array of focused spots utilising a multi-beam system was recently proposed (Lalithambigai *et al.* 2013; Prabakaran *et al.* 2014; Yiqiong Zhao *et al.* 2005; Cao *et al.* 2013). Dark hollow beams (DHBs) with zero central intensity have recently piqued the interest of many researchers due to their numerous uses in modern optics, atomic optics and binary optics. Several hollow laser beams with various intensity profiles have been introduced (Wang *et al.* 2004; Cai and Ge, 2006; Ito *et al.* 1996; Kuga *et al.* 1997; Cai *et al.* 2003; Mei and Zhao, *et al.* 2006a; 2006b; 2008). One such beam is the dark/anti-dark beam (DADB), which is theoretically introduced partially coherent diffraction-free modes (Ponomarenko *et al.* 2007). These beams can have intensity profiles with dips (or peaks) on a background to operate as nano-level atomic traps. Zhu *et al.* initially developed the approach of superposition of uncorrelated Bessel modes utilising holographic technology to construct DADBs (Zhu *et al.* 2019). A genuine cross-spectral density function criterion (Hyde and Avramov-Zumarovic, 2019) and a fully coherent class of dark/anti-dark paraxial modes named dark/anti-dark Bessel–Gaussian beams (DADGBs) have been proposed (Faroq and Belafhal, 2018). The propagation properties of these beams in a turbulent environment have recently been studied (Yaalou *et al.* 2019). The purpose of this study is to investigate the impact of a complex phase filter (CPF) on the focal characteristics of a tightly focused azimuthally polarised dark and anti-dark Gaussian (DADG) beam. It has been discovered that by properly designing a sophisticated phase filter for the incident DADG beam, one may produce several innovative focused patterns, such as focal ring splitting and multiple focal hole structures.

2. THEORY

The analysis was carried out using Richards and Wolf's Vectorial Diffraction approach, which is extensively utilised for high NA focusing systems with arbitrary incident polarisation. The incident azimuthally polarised beam's electric field distribution near the focussing is given by Richards and Wolf, 1959.

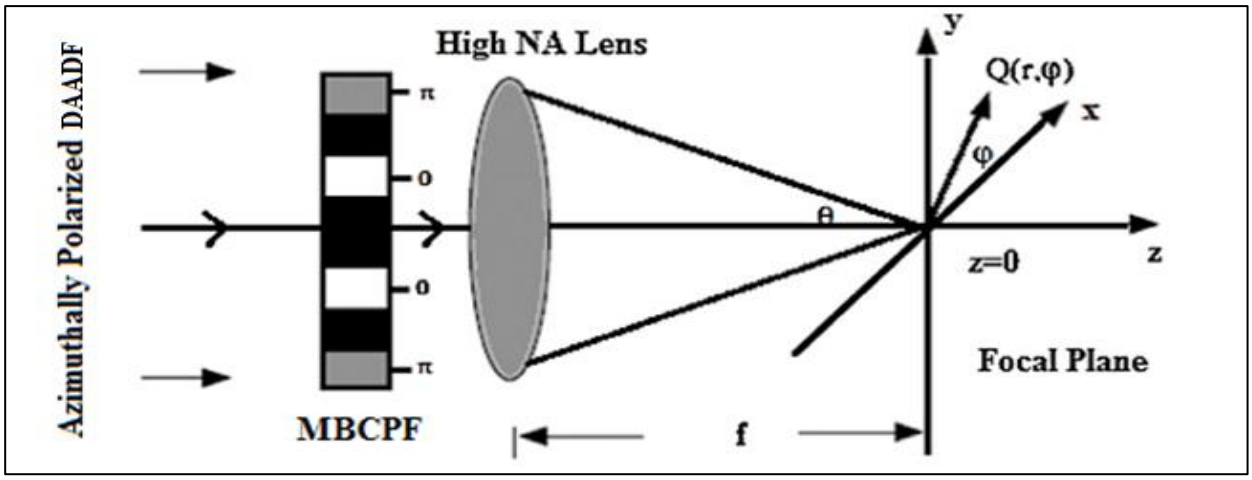

Fig. 1: Tight focusing of azimuthally polarized beam dark and anti-dark beam passes through a complex phase filter and is subsequently focused by a high-NA lens

$$E(r,\varphi,z)=\begin{bmatrix}E_r\\E_\varphi\\E_z\end{bmatrix}=\left[2A\int_0^{\alpha}\cos^{1/2}(\theta)\sin(\theta)\,\mathrm{A}(\theta)\,\mathrm{J}_1(kr\sin\theta)\,\mathrm{e}^{ikz\cos\theta}\right]d\theta\rightarrow(1)$$

where, A is the relative amplitude, θ_{max} = *arcsin (NA/n*) is the maximum aperture angle, (NA/n) is the ratio of numerical aperture (NA), n is the index of refraction between the lens and the sample and k is the wavenumber in free space. $J_n(\theta)$ denotes the nth order Bessel function and the function T*(θ)* describes the amplitude modulation. The analytical expression of the incident DADG beams in source plane z = 0, is given by (Yaalou *et al.* 2019),

$$E_0(r,z=0)=(1+\alpha\,\mathrm{J}_0(2\beta r))\exp\left(\frac{-r^2}{w_0^2}\right)\rightarrow(2)$$

J_0 is the zeroth order Bessel function of the first kind and α and β are arbitrary constants; β being real value and w_0 is the width of the Gaussian part. Obviously, for $\alpha=0$, the beam, governed by Eq. (2), reduces a conventional Gaussian beam. On the other hand, for α=-1 and 1, under these conditions, the incident beam field, established by Eq. (2), reduces to ADG and DG beams, respectively. For the objective that obeys the sine condition (Lin *et al.* 2011; Dehez *et al.* 2012), Eq. (2) stands to,

$$E_0(\theta)=\left(1+\alpha J_0\left(\frac{2\mu\sin\theta}{NA}\right)\right)\exp\left[-\frac{\sin^2\theta}{NA^2.w^2}\right]\rightarrow(3)$$

$w=w_0/\rho_0$ The relative waist width $\mu=\beta\rho_0$ is the ratio of the pupil radius $NA=\rho_0/f$ and $E_0(\theta)$ represents the amplitude variation of the DADG beam. Fig. 1 depicts the dedicated complex phase filter. The CPF is a phase and amplitude filter that consists of four radial belts. Multi-zone and amplitude filters are the most effective DOEs for lowering focus spot size and improving focal depth (Xu *et al.* 2007). The effect multi-belt complex phase filter on the input azimuthally polarized dark and anti-dark beam is evaluated by,

$$\mathrm{T}(\theta)=\begin{cases}0,\ for 0<\theta<\theta_1,\theta_2<\theta<\theta_3,\\1,\ for\theta_1<\theta<\theta_2,\\-1\,for\theta_3<\theta<\theta_{\max}\end{cases}\rightarrow(4)$$

In this example, it has been assumed that the typical global-search-optimization methodology optimises the collection of four angles needed to construct specialised focused patterns. Based on this technique, we select one structure from all possibilities (with random values for θ_1 to θ_3) and simulate its focusing properties using Vector Diffraction theory. If the structure created a sub-wavelength single focus spot and met the limiting requirements of the generated focal spot segment having a Full-Width Half Maximum (FWHM) of less than 0.5λ, it was chosen as the initial structure for the optimization operations. In the next phases, the authors continued to vary θ of one chosen zone to produce various focused spot segments while

keeping in mind the limiting constraints that the FWHM of each generated focal spot was less than 0.5λ and that the focal segment contained at least five, three, or two such focal spots.

3. RESULTS AND DISCUSSION

The integration of Eq. (1) was done numerically using the parameters λ as 1 and NA of the objective as 0.9. Here, for simplicity, it has been assumed that the refractive index, n = 1 and A = 1; for all calculation the length unit was normalized to λ and the energy density was normalized to unity. Fig. 2. illustrates the evolution of three-dimensional light intensity distribution of the high NA lens for the incident phase-modulated dark hollow beam. The set of complex phase filter angles for the generation of multiple focal holes are θ_1 = 50.90°, θ_2 = 54.85°, θ_3 = 60.83° and θ_{max} = 64.19°.

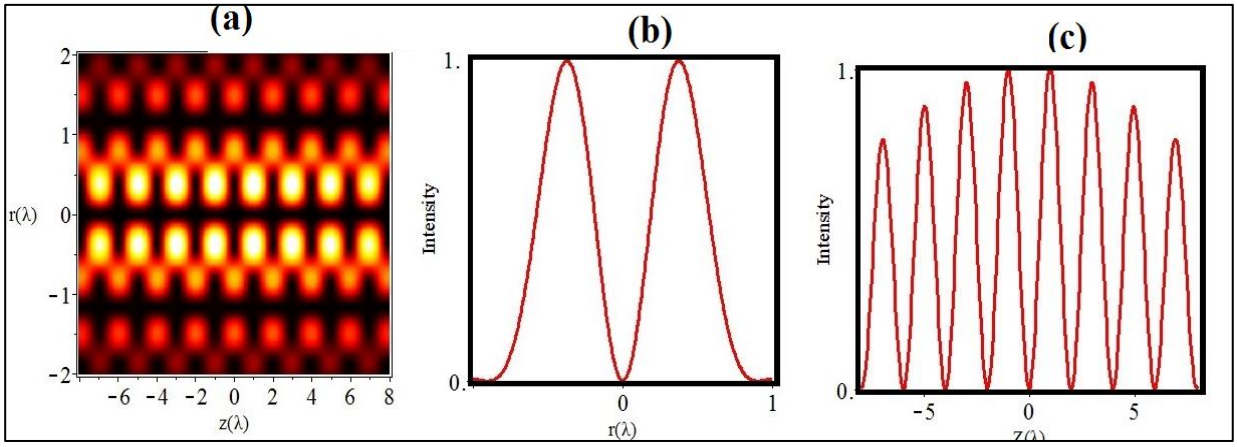

Fig. 2: (a) Total intensity distribution in the r−z plane for Phase-modulated Azimuthally polarized Dark hollow Gaussian beam (α = 1), (b) Intensity distribution of the radial direction at r = 0.35λ and c) Axial intensity distribution, z =1.1λ

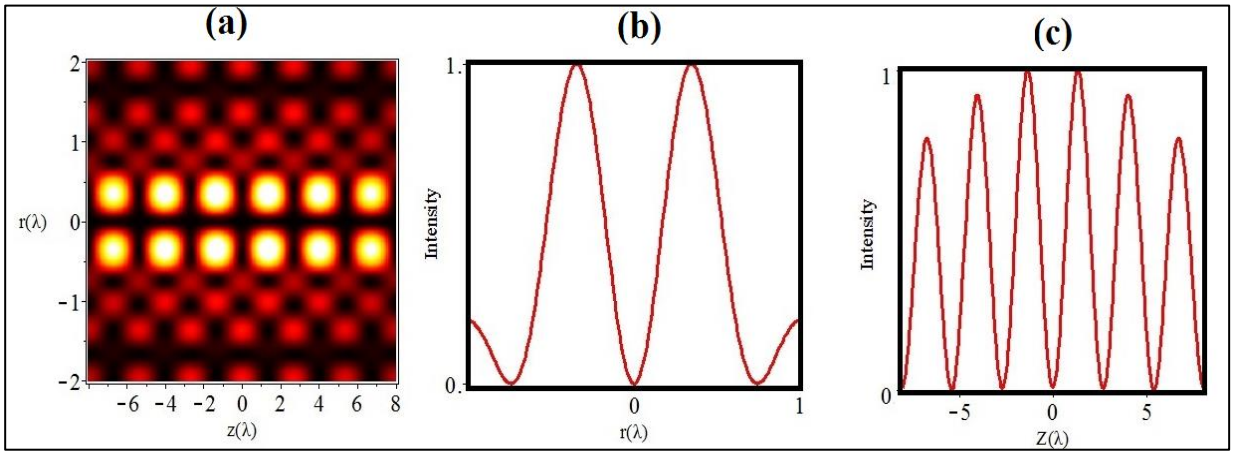

Fig. 3: (a) Total intensity distribution in the r−z plane, (b) Intensity distribution in the radial direction at r = 0.35λ and c) axial intensity distribution, z = 1.1λ

Fig. 2 (a) illustrates the splitting of focal hole segment generated by the high NA lens for the phase modulated dark beam. It was observed from Fig. 2 (a) that the generated focal hole segment was uniformly separated in the focal region and each focal hole has the focal depth around 2.8λ measured at r = 0.3λ and the axial distance of separation of each focal hole was 1.8λ, as shown in Fig. 2 (c). It was observed from Fig. 2 (b) that the FWHM of each ring was 0.37λ.

Fig. 3 (a) depicts the array of focal hole segments generated by the high NA lens for the CPF with angles optimized as θ_1 = 50.90°, θ_2 = 56.85°, θ_3 = 60.83° and θ_{max} = 64.19°. From Fig. 3 (a-b), it has been observed that the focal holes segment contained 6 focal holes of almost uniform intensity, each having FWHM of 0.362λ and were axially separated by the distance of 1.6λ. The on axial intensity of the generated focal hole segment, calculated at r = 0.3λ, has been shown in Fig. 4 (c) and it was observed that the DOF of each focal hole was 2λ.

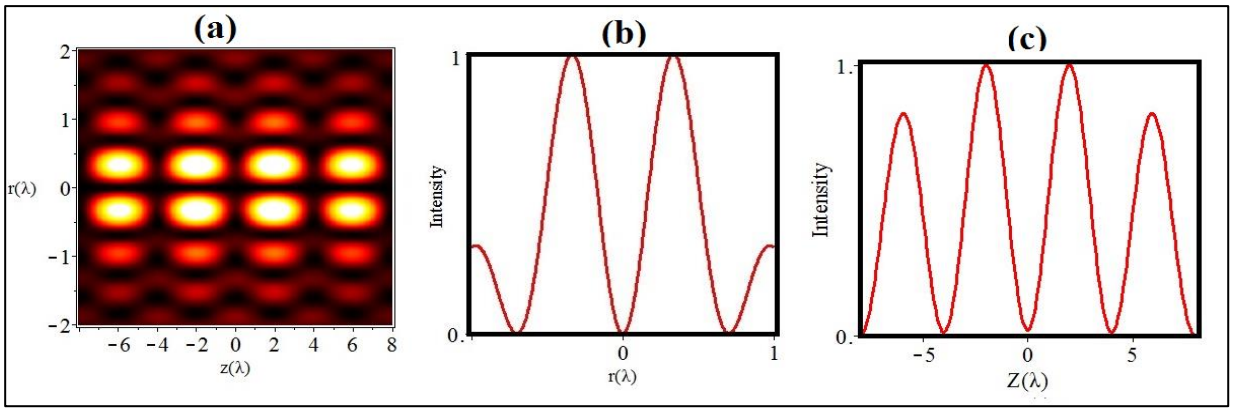

Fig. 4: (a) Total intensity distribution in the r–z plane, (b) Intensity distributions of the radial direction at r = 0.35λ and c) Axial intensity distribution, z = 1.1λ

Fig. 4 (a-c). shows the generation of four focal hole pattern by CPP optimized with angles θ1=50.90°, θ2= 56.85° and θ3= 60.83°, θ_{max}= 64.19°. From the figure we observed that the generated focal holes segment contains four focal holes and the light intensities of these four focal holes are approximately equal and each having FWHM of 0.345λ and are separated by axial distance of 2λ between them. It is observed that each focal hole having focal depth around 2.8λ as measured from intensity distribution at r = 0.3λ and is shown in Fig. 5 (c).

Fig. 5 (a) shows the total tow dimensional intensity distribution of the axially extended focal hole generated by the proposed high NA lens with dedicated CPF. It was observed from Fig. 8.5 (c) that the generated focal hole extends up to 3λ with uniform axial intensity. From fig. 5 (b) the FWHM of the generated focal hole is measured as 0.332λ. The set of three angles of the CPP optimized to achieve the above mentioned focal hole segment are θ_1=50.90°, θ_2= 56.85° and θ_3= 58.83°. θ_{max}= 64.19°. The angle of the CPP optimum for the production of focal hole segment for incident azimuthally polarised Dark and Anti-Dark Hollow Gaussian beams is shown in Table 1. A subwavelength scale long focal depth like this could be useful in optical, biological, and atmospheric sciences.

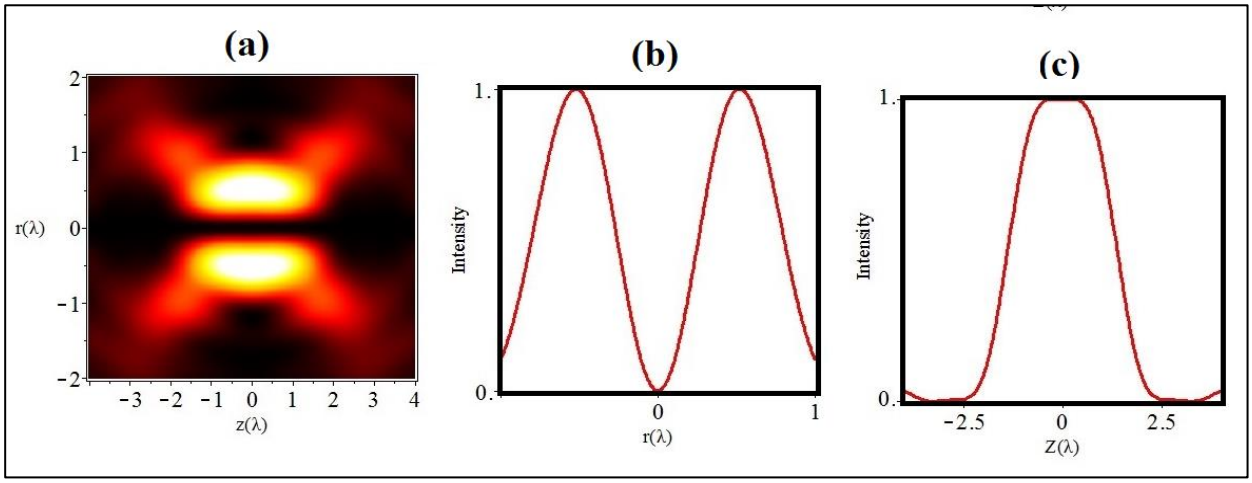

Fig. 5: (a) Total intensity distribution in the r–z plane for Phase-modulated Azimuthally polarized Anti-dark hollow Gaussian beam (α = -1), (b) Intensity distribution of the radial direction at r = 0.35λ and c) Axial intensity distribution, z = 1.1λ.

Table 1. FWHM and DOF values of focal holes generated for different beam parameter α and complex phase filter

S. No.	DADG beam parameter	Optimized angle of CPF	Number of Focal holes	FWHM (λ)	DOF (λ)	Axial separation (λ)
1	+1	$\theta_1 = 50.90^\circ$, $\theta_2 = 54.85^\circ$, $\theta_3 = 60.83^\circ$ and $\theta_{max} = 64.19^\circ$	8	0.37	2.8	1.8
2	+1	$\theta_1 = 50.90^\circ$, $\theta_2 = 56.85^\circ$, $\theta_3 = 58.83^\circ$ and $\theta_{max} = 64.19^\circ$	6	0.36	2	1.6
3	+1	$\theta_1 = 46.90^\circ$, $\theta_2 = 56.85^\circ$, $\theta_3 = 60.83^\circ$ and $\theta_{max} = 64.19^0$	4	0.34	2.8	2
4	-1	$\theta_1 = 50.90^\circ$, $\theta_2 = 56.85^\circ$, $\theta_3 = 60.83^\circ$ and $\theta_{max} = 64.19^\circ$	1	0.33	3	Uniform axial intensity

4. CONCLUSION

The Vector Diffraction theory was applied to investigate the theoretical focusing of Azimuthally polarised Dark and Anti-dark Gaussian (DADG) beams passing through a high numerical-aperture (NA) lens. It has been found that many innovative focus patterns can be generated, such as focal hole segments with a variable number of focal holes with uniform intensity distribution and axially extended sub-wavelength focal holes, among others. It has also been discovered that the number of focal holes and the axial distance between them may be adjusted by adjusting the phase of the incident azimuthally polarised light beam with DADG (dark and anti-dark Gaussian) distributions. Since it can be done accurately and controllably, a tuneable multiple focus hole with variable axial distance is an effective tool for optical trapping of low refractive index particles.

FUNDING

This research received no specific grant from any funding agency in the public, commercial, or not-for-profit sectors.

CONFLICTS OF INTEREST

The authors declare that there is no conflict of interest.

REFERENCES

Cai, Y. and Ge, D., Propagation of various dark hollow beams through an aperture paraxial ABCD optical system, *Phys. Lett. A.*, 357(1), 72–80 (2006). https://dx.doi.org/10.1016/j.physleta.2006.04.022

Cai, Y., Lu, X. and Lin, Q., Hollow Gaussian beam and its propagation properties, *Opt. Lett.*, 28(13), 1084–1086 (2003). https://dx.doi.org/10.1364/OL.28.001084

Cao, J., Chen, Q. and Guo, H., Creation of a controllable three dimensional optical chain by TEM01mode radially polarized Laguerre–Gaussian beam, *Optik.*, 124(15), 2033–2036 (2013). https://dx.doi.org/10.1016/j.ijleo.2012.06.057

Cizmar, T., Romero, L. C. D., Dholakia, K. and Andrews, D. L., Multiple optical trapping and binding: new routes to self-assembly, *J. Phys. B: Atomic, Molecular and Optical Physics*, 43(10), 102001 (2010). https://dx.doi.org/10.1088/0953-4075/43/10/102001

Dehez, H., April, A. and Piché, M., Needles of longitudinally polarized light: guidelines for minimum spot size and tunable axial extent, *Opt. Express*, 20(14) , 14891–14905 (2012). https://dx.doi.org/10.1364/OE.20.014891

Faroq, S. and Belafhal, A., Conical difraction of dark and antidark beams modulated by a Gaussian profle in biaxial crystals, *Optik.*, 154, 344–353 (2018). https://dx.doi.org/10.1016/j.ijleo.2017.10.049

Friedman, N., Kaplan, A. and Davidson, N., Dark optical traps for cold atoms, *Adv. At. Mol. Opt. Phys.*48, 99–151 (2002). https://dx.doi.org/10.1016/S1049-250X(02)80007-6

Grimm, R., Weidemuller, M. and Ovchinnikov, Y. B., Optical dipole traps for neutral atoms, *Adv. Atom. Mol. Opt. Phys*.,42, 95–170 (2000). https://dx.doi.org/10.1016/S1049-250X(08)60186-X

Hyde, M. W. and Avramov-Zumarovic, S., Generating dark and antidark beams using the genuine cross spectral density function criterion, *J. Opt. Soc. Am. A.*, 36(6), 1058–1063 (2019). https://dx.doi.org/10.1364/JOSAA.36.001058

Ito, H., Nakata, T., Sakaki, K., Ohtsu, M., Lee, K. I. and Jhe, W., Laser spectroscopy of atoms guided by evanescent waves in micron-sized hollow optical fibers, *Phys. Rev. Lett.*, 76, 4500–4503 (1996). https://dx.doi.org/10.1103/PhysRevLett.76.4500

Kuga, T., Torii, Y., Shiokawa, N., Hirano, T., Shimizu, Y. and Sasada, H., Novel optical trap of atoms with a doughnut beam, *Phys. Rev. Lett.*, 78, 4713–4716 (1997). https://dx.doi.org/10.1103/PhysRevLett.78.4713

Lalithambigai, K., Saraswathi, R. C., Anbarasan, P. M., Rajesh, K. B. and Jaroszewicz, Z., Generation of multiple focal hole segments using double-ring shaped azimuthally polarized beam, *J. Atomic Mol. Phy*., 01–04 (2013). https://dx.doi.org/10.1155/2013/451715

Lalithambigai, K., Suresh, P., Ravi, V., Prabakaran, K., Jaroszewicz, Z., Rajesh, K. B., Anbarasan, P. M. and Pillai, T. V., Generation of sub wavelength super-long dark channel using high NA lens axicon, *Opt. Lett.*, 37(6), 999–1001 (2012). https://dx.doi.org/10.1364/OL.37.000999.

Lin, J., Yin, K., Li, Y. and Tan, J. B., Achievement of longitudinally polarized focusing with long focal depth by amplitude modulation, *Opt. Lett*., 36(7), 1185–1187 (2011). https://dx.doi.org/10.1364/OL.36.001185

Mei, Z. and Zhao, D., Controllable elliptical dark-hollow beams, *J. Opt. Soc. Am. A.*, 23, 919–925 (2006a). https://dx.doi.org/10.1364/JOSAA.22.001898

Mei, Z. and Zhao, D., Generalized M2 factor of hard-edged difracted controllable dark-hollow beams, *Opt. Commun*., 263(2), 261–266 (2006b). https://dx.doi.org/10.1016/j.optcom.2006.01.039

Mei, Z. and Zhao, D., Non-paraxial propagation of controllable dark-hollow beams, *J. Opt. Soc. Am. A.*, 25(3), 537–542 (2008). https://dx.doi.org/10.1364/JOSAA.25.000537

Ponomarenko, S. A., Huang, W. and Cada, M., Dark and antidark diffraction-free beams, *Opt. Lett*., 32(17), 2508–2510 (2007). https://dx.doi.org/10.1364/OL.32.002508

Prabakaran, K., Rajesh, K. B., Pillai, T. V. S., Chandrasekaran, R. and Jaroszewicz, Z., Generation of multiple focal spot and focal hole of sub wavelength scale using phase modulated LG (1,1) beam, *Optik*, 124(21), 5086–5088 (2014). https://dx.doi.org/10.1016/j.ijleo.2013.03.068

Richards, B. and Wolf, E., Electromagnetic diffraction in optical systems, II. Structure of the image field in an aplanatic system, *Proc. R. Soc. Lond. A Math. Phys. Sci.*, 253, 358–379 (1959). https://dx.doi.org/10.1098/rspa.1959.0200

Tian, B. and Pu, J., Tight focusing of a double-ring-shaped, azimuthally polarized beam, *Opt. Lett*., 36(11), 2014–2016 (2011). https://dx.doi.org/10.1364/OL.36.002014

Wang, Z., Lin, Q. and Wang, Y.: Control of atomic rotation by elliptical hollow beam carrying zero angular momentum, *Opt. Commun*., 240(4), 357–362 (2004). https://dx.doi.org/10.1016/j.optcom.2004.06.044

Watanabe, T., Iketaki, Y., Omatsu, T., Yamamoto, K., Sakai, M. and Fuji, M., Two point separation in super-resolution fluorescence microscope based on up-conversion fluorescence depletion technique. *Opt. Express*, 11(24), 3271–3276 (2003). https://dx.doi.org/10.1364/OE.11.003271

Xu, Y., Singh, J., Sheppard, C. J. R. and Chen, N., Ultra long high resolution beam by multi-zone rotationally symmetrical complex pupil filter, *Opt. Express*, 15(10), 6409–6413 (2007). https://dx.doi.org/10.1364/OE.15.006409

Yaalou, M., El Halba, E. M., Hricha, Z. and Belafhal, A., Propagation characteristics of dark and antidark Gaussian beams in turbulent atmosphere, *Opt. Quantum Electron.*, (2019). https://dx.doi.org/10.1007/s11082-019-1972-z

Yaalou, M., El Halba, E. M., Hricha, Z. and Belafhal, A., Transformation of double-half inverse Gaussian hollow beams into superposition of finite airy beams using an optical airy transform, *Opt. Quantum Electron*., 51, 64–75 (2019). https://dx.doi.org/10.1007/s11082-019-1775-2

Yiqiong Zhao, Qiwen Zhan, Yanli Zhang, Yong-Ping Li, Creation of a threedimensional optical chain for controllable particle delivery, *Opt. Lett*., 30(8), 848–850 (2005). https://dx.doi.org/10.1364/OL.30.000848

Zha, Y., Wei, J., Wang, H, and Gan, F., Creation of an ultra-long depth of focus super resolution longitudinally polarized beam with a ternary optical element, *J. Opt.* 15(7), 075703 (2013). https://dx.doi.org/10.1088/2040-8978/15/7/075703

Zhu, X., Wang, F., Zhao, C., Cai, Y. and Ponomarenko, S. A., Experimental realization of dark and anti dark difraction-free beams, *Opt. Lett*., 44, 2260–2263 (2019). https://dx.doi.org/10.1364/OL.44.002260